Développement d'un modèle dispersif hyperbolique pour les vagues côtières et implémentation dans Tolosa.

Arnaud Duran, Maria Kazakova, Yen-Chung Hung, Rémy Baraille, Frédéric Couderc, Jean-Paul Vila, Julien Chauchat, Gaël Loïc Richard

Développement d'un modèle dispersif hyperbolique pour les vagues côtières et implémentation dans Tolosa

Derivation of a disspersive-hyperbolic model for coastal waves et its numerical implementation

Y.-C. Hung[(1)], M. Kazakova[(1)], G. L. Richard[(2)], J. Chauchat[(3)], R. Baraille[(5,6)], F. Couderc[(5)], A. Duran[(4)], J.-P. Vila[(5)]

yen-chung.hung@univ-smb.fr

[(1)] Univ. Grenoble Alpes, Univ. Savoie Mont Blanc, CNRS, LAMA, Chambéry
[(2)] Univ. Grenoble Alpes, INRAE, UR ETNA, Grenoble
[(3)] Univ. Grenoble Alpes, CNRS, Grenoble INP, LEGI, Grenoble
[(4)] Univ. Claude Bernard Lyon 1, ICJ, Lyon
[(5)] Univ. de Toulouse, CNRS, IMT, INSA, Toulouse
[(6)] SHOM - Service Hydrographique et Océanographique de la Marine, France.

Summary

In this study, we propose a new hyperbolic model with the same dispersive properties as the classical Serre-Green-Naghdi model capable to capture the wave breaking phenomenon. The hyperbolisation of the equations is based on taking into account the finite character of the sound speed and thus the compressibility of the sea water. The method therefore involves introducing acoustic energy into the system. In the case of coastal waves, the effects of static compressibility are negligible. The resulting model is then a hyperbolic approximation of the Serre-Green-Naghdi equations. The modelling of breaking waves is obtained by adapting to this pseudo-compressible approach the depth-averaging method of Large-Eddy Simulations (LES) where the small scale turbulence is modelled by a turbulent viscosity, whereas the large scales are taken into account in the model by an anisotropic tensor variable called enstrophy.

Résumé

Dans cette étude, nous proposons un nouveau modèle hyperbolique avec les mêmes propriétés dispersives que le modèle classique de Serre-Green-Naghdi capable de capturer le phénomène de déferlement des vagues. L'hyperbolisation des équations est basée sur la prise en compte du caractère fini de la vitesse du son et donc de la compressibilité de l'eau de mer. La méthode implique donc d'introduire une énergie acoustique dans le système. Dans le cas des vagues côtières, les effets de compressibilité statique sont négligeables. Le modèle obtenu est alors une approximation hyperbolique des équations de Serre-Green-Naghdi. La modélisation du déferlement est obtenue par l'adaptation à cette approche pseudo-compressible de la méthode de moyenne sur la profondeur des équations de la simulation des grandes échelles de la turbulence (SGS) où les petites échelles de la turbulence sont modélisées par une viscosité turbulente, en revanche les grandes échelles sont prises en compte dans le modèle par une variable tensorielle anisotrope appelée enstrophie.

In the current environmental context, in view of the issues related to the increase in the frequency of extreme events such as severe storms and flooding, the precise and operational

description of the coastal flows is essential. Similarly, the phenomenon of coastal erosion, aggravated by climate change, requires the development of effective prevention models and tools. In spite of constant technical progress, the direct resolution of the Navier-Stokes equations is still out of reach from an operational point of view. In this context, the interest is focused on simplified models, less expensive numerically and allowing to get closer to real time simulations. This is where depth-averaged models such as the Shallow Water equations, or more precise models such as the weakly dispersive Boussinesq equations or the fully nonlinear Serre-Green-Naghdi (SGN) equations come into play. The latter are often used in coastal oceanography because they allow to capture the dispersion and the strong non-linearities induced by the bottom variations at the approach of the shore. However, the obstacles associated with the numerical implementation of these models are numerous. One of the main difficulties associated with the dispersive equations is the presence of an elliptic-type operator, which requires the inversion of a global linear system. This is a serious obstacle since it takes a large part of the computation time. Furthermore, the treatment of the elliptical operator requires a specific choice of discrete formulations in order to ensure the stability and the well-posedness of the problem.

In the last few years, new methods have emerged that allow to partly tackle these difficulties. They are based on hyperbolic models consisting of relaxed versions of the SGN equations. One can for instance refer to the recent work [6] where the derivation of the equations relies on an extended Lagrangian variational principle, or [4], [5], [10] where a compressible version of the dispersive model for water waves has been derived. The hyperbolic nature of those models provides an appropriate framework for the construction of a numerical scheme and allows to get rid of most of the limitations of the existing strategies for SGN equations.

However those models (dispersive or hyperbolic) are derived in a conservative context, meaning that they conserve mechanical energy, and therefore they are not capable to capture the dissipation when breaking of waves occurs. The different methodologies proposed in the literature to describe wave-breaking fall into two categories. The first strategy consists in adding an artificial viscosity term in the mass and/or momentum equations (see e.g. [9]). The second strategy (used for exemple in [13], [2]), commonly called switching approach, consists in suppressing the dispersive terms in the vicinity of breaking waves, leaving only the hyperbolic part of the model (Shallow Water) to be locally resolved. This approach allows to model the breaking waves as shocks and to use the natural dissipation through the shock. Although these strategies allow to describe the breaking process they requires a calibration of a large number of parameters, moreover, the discontinuities introduced in the model by the addition or deletion of terms generate transition instabilities, which can propagate and considerably deteriorate the quality of the approximations. A new approach has recently been proposed in [8], [11] : it generalizes the classical SGN equations by taking into account wave-breaking through a new variable (scalar in 1D and tensor in 2d) related to the turbulent energy, called enstrophy. However, the proposed models have a similar structure to the SGN equations and implies therefore a time-consuming treatement of the elliptic step.

In the present study we aim to derived a hyperbolic dispersive model capable to describe breaking waves. We note that the approach proposed in [8] to describe wave breaking can be used without compromising the derivation proposed in [4, 5, 10], and therefore the hyperbolic structure of the system can be obtained. This model is intended to be implemented in the TOLOSA code developed for the forecasting and prevention of the risk of marine submersion in association with the SHOM and Météo France. Also, the consideration of turbulence also opens up prospects for coupling with morphodynamic

models for the description of erosion and sediment transport. This constitutes a subject of a future research.

I – Derivation

Let's consider a two-dimensional flow over a time-independent bottom b. The velocity components are denoted as u, w for the Ox, Oz directions, respectively. Let $Z = Z(x,t)$ be the free-surface elevation and $h = Z - b$ the depth. Figure 1 gives a demonstration of the setup.

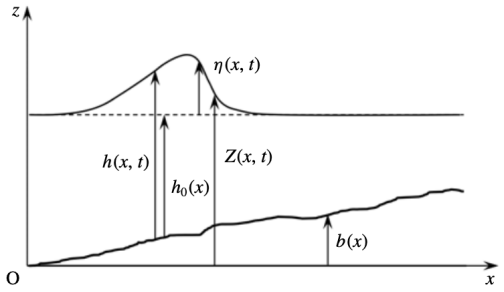

FIGURE 1 – Definition sketch

Following [8] we begin with mimicking the large-eddy simulation method that decomposes the velocity field $\boldsymbol{v} = (u, w)^\top$ into a filtered velocity field $\overline{\boldsymbol{v}}$ and a residual term $\boldsymbol{v}^r$

$$\boldsymbol{v} = \overline{\boldsymbol{v}} + \boldsymbol{v}^r.$$

The filtered velocity field $\overline{\boldsymbol{v}}$ here includes a large scale turbulence. The filter is then applied to the Navier-Stokes equation of incompressible Newtonian fluid of density ρ and kinematic viscosity ν.

$$\frac{\partial \bar{u}}{\partial x} + \frac{\partial \bar{w}}{\partial z} = 0, \tag{1a}$$

$$\frac{\partial \bar{u}}{\partial t} + \frac{\partial \bar{u}^2}{\partial x} + \frac{\partial \bar{u}\bar{w}}{\partial z} = -\frac{1}{\rho}\frac{\partial p}{\partial x} + \frac{1}{\rho}\left(\frac{\partial A^r_{xx}}{\partial x} + \frac{\partial A^r_{xz}}{\partial z}\right) + \nu\left(\frac{\partial^2 \bar{u}}{\partial x^2} + \frac{\partial^2 \bar{u}}{\partial z^2}\right), \tag{1b}$$

$$\frac{\partial \bar{w}}{\partial t} + \frac{\partial \bar{u}\bar{w}}{\partial x} + \frac{\partial \bar{w}^2}{\partial z} = -g - \frac{1}{\rho}\frac{\partial p}{\partial z} + \frac{1}{\rho}\left(\frac{\partial A^r_{xz}}{\partial x} + \frac{\partial A^r_{zz}}{\partial z}\right) + \nu\left(\frac{\partial^2 \bar{w}}{\partial x^2} + \frac{\partial^2 \bar{w}}{\partial z^2}\right), \tag{1c}$$

where $A^r_{xx},\ A^r_{xz},\ A^r_{zz}$ are part of the stress tensor that has the form

$$A^r_{xx} = 2\nu_T \frac{\partial u}{\partial x},\ A^r_{zz} = -A^r_{xx},\ A^r_{xz} = \nu_T\left(\frac{\partial u}{\partial z} + \frac{\partial w}{\partial x}\right) \tag{2}$$

with ν_T is the turbulent viscosity for the small-scale turbulence.

The model is derived by averaging the filtered equations over the fluid depth and neglecting all the terms of high order with respect to the shallowness parameter

$$\varepsilon = \frac{h_0}{L} \ll 1,$$

where L, h_0 are the horizontal and vertical characteristic lengths, respectively. The boundary conditions are

– No-penetration condition at the bottom $w(b) = u(b)\dfrac{db}{dx}$

– Kinematic and dynamic condition at the free surface

$$w(Z) = \frac{\partial h}{\partial t} + u(Z)\frac{\partial Z}{\partial x} \text{ and } (\boldsymbol{\sigma}\cdot\boldsymbol{n})(Z) = 0, \tag{3}$$

In the derivation of our model, we further assume that there is no surface tension and no shear stress at the free surface. We decompose the filtered horizontal velocity as

$$\bar{u}(x,z,t) = U(x,t) + u'(x,z,t), \tag{4}$$

where U is a mean velocity and u' represents the deviation part. The hypothesis of weakly turbulent flow from Teshukov [12] assumes that the order of the vertical deviation u' is of $O(\varepsilon)$. Furthermore, the pressure p is separated into the sum of a hydrostatic pressure p_H and a non-hydrostatic pressure p_N

$$p = p_H + p_N = \rho g(Z - z) + p_N. \tag{5}$$

Then, we apply the following scaling to the system of filtered equations

$$\tilde{x} = \frac{x}{L},\ \tilde{z} = \frac{z}{h_0},\ \tilde{t} = \varepsilon t\sqrt{\frac{g}{h_0}},\ \tilde{h} = \frac{h}{h_0},\ \tilde{b} = \frac{b}{h_0},\ \tilde{u} = \frac{\bar{u}}{\sqrt{gh_0}},\ \tilde{w} = \frac{\bar{w}}{\varepsilon\sqrt{gh_0}},\ \tilde{p} = \frac{p}{\rho g h_0},$$

$$\tilde{Z} = \frac{Z}{h_0},\ \tilde{A}^r_{xx} = \frac{A^r_{xx}}{\varepsilon^2\rho g h_0},\ \tilde{A}^r_{zz} = \frac{A^r_{zz}}{\varepsilon^2\rho g h_0},\ \tilde{A}^r_{xz} = \frac{A^r_{xz}}{\varepsilon\rho g h_0}.$$

By depth-averaging the dimensionless filtered equation (1), the continuity equation takes the form

$$\frac{\partial\tilde{h}}{\partial\tilde{t}} + \frac{\partial\tilde{h}\tilde{U}}{\partial\tilde{x}} = 0, \tag{6}$$

and the momentum equation Ox (1b) becomes

$$\frac{\partial\tilde{h}\tilde{U}}{\partial\tilde{t}} + \frac{\partial}{\partial\tilde{x}}\left(\tilde{h}\tilde{U}^2 + \frac{\tilde{h}^2}{2} + \varepsilon^2\tilde{h}\left\langle\tilde{u}'^2\right\rangle + \varepsilon^2\int_{\tilde{b}}^{\tilde{Z}}\tilde{p}_N d\tilde{z} - \varepsilon^2 2\tilde{\nu}_T\tilde{h}\frac{\partial\tilde{U}}{\partial\tilde{x}}\right) = -\tilde{p}(b)\frac{\partial\tilde{b}}{\partial\tilde{x}} \tag{7}$$

Then, following [8] we define the enstrophy as

$$\tilde{\varphi} := \frac{\langle\tilde{u}'^2\rangle}{\tilde{h}^2}, \tag{8}$$

and following [10] the depth-averaged non-hydrostatic pressure as

$$\tilde{P} = \frac{1}{\tilde{h}}\int_{\tilde{b}}^{\tilde{Z}}\tilde{p}_N d\tilde{z}. \tag{9}$$

This definition of P allows the whole system to be hyperbolic. Note that to keep the enstrophy terms in our model, we should keep all the terms up to the order of $O(\varepsilon^2)$. In this case, the Oz-momentum equation (1c) becomes

$$\frac{\partial\tilde{h}\tilde{W}}{\partial\tilde{t}} + \frac{\partial\tilde{h}\tilde{U}\tilde{W}}{\partial\tilde{x}} = \tilde{p}_N(b) \tag{10}$$

To obtain $\tilde{p}_N(b)$, we first use the continuity equation (1a)

$$\frac{\partial \tilde{w}}{\partial \tilde{z}} = -\frac{\partial \tilde{u}}{\partial \tilde{x}} = -\frac{\partial \tilde{U}}{\partial \tilde{x}} - \varepsilon \frac{\partial \tilde{u}'}{\partial \tilde{x}} \tag{11}$$

Integrating (11) from $\tilde{b}$ to $\tilde{z}$ with respect to $\tilde{z}$, we have

$$\tilde{w} = (\tilde{b} - \tilde{z})\frac{\partial \tilde{U}}{\partial \tilde{x}} + \tilde{U}\frac{\partial \tilde{b}}{\partial \tilde{x}} + O(\varepsilon). \tag{12}$$

Then the depth-averaged vertical velocity reads

$$\tilde{W} = -\frac{\tilde{h}}{2}\frac{\partial \tilde{U}}{\partial \tilde{x}} + \tilde{U}\frac{\partial \tilde{b}}{\partial \tilde{x}} + O(\varepsilon). \tag{13}$$

Substituting (12) and (13) into the Oz-momentum equation (1c) and integrating from $\tilde{z}$ to $\tilde{Z}$ yields

$$\begin{aligned}\tilde{p}_N(\tilde{z}) = \left(\frac{(\tilde{b}-\tilde{z})^2}{2} - \frac{\tilde{h}^2}{2}\right)\left(\frac{\partial^2 \tilde{U}}{\partial \tilde{t}\partial \tilde{x}} + \frac{\partial}{\partial \tilde{x}}\left(\tilde{U}\frac{\partial \tilde{U}}{\partial \tilde{x}}\right) - 2\left(\frac{\partial \tilde{U}}{\partial \tilde{x}}\right)^2\right) \\ + (\tilde{Z} - \tilde{z})\ddot{\tilde{b}} + \tilde{A}^r_{zz} + O(\varepsilon),\end{aligned}$$

where $\dot{b} = \dfrac{Db}{Dt} = \dfrac{\partial b}{\partial t} + U\dfrac{\partial b}{\partial x}$ and $\ddot{b} = \dfrac{D\dot{b}}{Dt}$. Then, we have the following relation between $\tilde{P}$ and $\tilde{p}_N(b)$

$$\tilde{p}_N(b) = \frac{3}{2}\tilde{P} + \frac{\tilde{h}}{4}\ddot{\tilde{b}} + 3\tilde{\nu}_T\frac{\partial \tilde{U}}{\partial \tilde{x}} + O(\varepsilon). \tag{14}$$

Combining (6), (7), and (10) with the definitions of φ and P ((8), (9)) and relation (14), we finally have the three dimensinal equations

$$\frac{\partial h}{\partial t} + \frac{\partial hU}{\partial x} = 0 \tag{15a}$$

$$\begin{aligned}\frac{\partial hU}{\partial t} + \frac{\partial}{\partial x}\left(hU^2 + \frac{gh^2}{2} + h^3\varphi + hP - 2\nu_T h\frac{\partial U}{\partial x}\right) \\ = -gh\frac{\partial b}{\partial x} - \left(\frac{3}{2}P + \frac{h}{4}\ddot{b} + 3\nu_T\frac{\partial U}{\partial x}\right)\frac{\partial b}{\partial x}\end{aligned} \tag{15b}$$

$$\frac{\partial hW}{\partial t} + \frac{\partial hUW}{\partial x} = \frac{3}{2}P + \frac{h}{4}\ddot{b} + 3\nu_T\frac{\partial U}{\partial x} \tag{15c}$$

Note that we introduce two additional variables P and φ. To close the system, we consider the acoustic energy equation

$$\begin{aligned}&\frac{\partial}{\partial t}\left(\frac{\rho u^2}{2} + \frac{\rho w^2}{2} + \rho g z + \rho e_a\right) \\ &\quad + \frac{\partial}{\partial x}\left[\left(\frac{\rho u^2}{2} + \frac{\rho w^2}{2} + \rho g z + \rho e_a + p - A^r_{xx}\right)u - A^r_{xz}w\right] \\ &\quad + \frac{\partial}{\partial z}\left[\left(\frac{\rho u^2}{2} + \frac{\rho w^2}{2} + \rho g z + \rho e_a + p - A^r_{zz}\right)w - A^r_{xz}u\right] = -P^r,\end{aligned} \tag{16}$$

where e_a is the acoustic energy and P^r is a dissipative term. By depth-averaging (16) over the depth, we end up having the coupled equation for enstrophy and the mean acoustic energy

$$\begin{aligned}&\frac{h^2}{2}\left(\frac{\partial h\varphi}{\partial t}+\frac{\partial hU\varphi}{\partial x}\right)+\frac{\partial h\langle e_a\rangle}{\partial t}+\frac{\partial hU\langle e_a\rangle}{\partial x}\\&\quad=-h\left\langle P^r\right\rangle-\left(hP-2\nu_T h\frac{\partial U}{\partial x}\right)\frac{\partial U}{\partial x}-2\left(P+2\nu_T\frac{\partial U}{\partial x}\right)(W-\dot{b}).\end{aligned}\tag{17}$$

We apply the same postulate used in [10] for the averaged acoustic energy $\langle e_a\rangle=\dfrac{P^2}{2a^2}$, where a is the sound velocity which is assumed to be constant. Following [8], we introduce the empirical expressions for the dissipation term $\langle P^r\rangle$ and the turbulent viscosity ν_T

$$\langle P^r\rangle=\frac{C_r}{2}h^2\varphi^{3/2},\quad \nu_T=\frac{h^2\sqrt{\varphi}}{R},\tag{18}$$

where C_r is a dimensionless quantity and R can be interpreted as a turbulent Reynolds number related to the small-scale turbulence.

For the shoaling zone, where wave breaking does not occur, the assumption $\varphi\equiv 0$ is appropriate. Then the equation for averaged non-hydrostatic pressure P reads

$$\frac{\partial hP}{\partial t}+\frac{\partial hUP}{\partial x}=-a^2\left(h\frac{\partial U}{\partial x}+2W-2\dot{b}\right).\tag{19}$$

Consequently, we can obtain the equation for the enstrophy φ

$$\frac{\partial h\varphi}{\partial t}+\frac{\partial hU\varphi}{\partial x}=-C_r h\varphi^{3/2}+\frac{4h\sqrt{\varphi}}{R}\left(\frac{\partial U}{\partial x}\right)^2-\frac{8\sqrt{\varphi}}{R}\frac{\partial U}{\partial x}\left(W-\dot{b}\right).\tag{20}$$

The equations (15) as well as (19) and (20) are the final system of equations. Under the mild slope condition (we neglect the terms involving $\partial_x b$ of order larger than $O(\varepsilon^3)$), we have

$$\begin{aligned}&\frac{\partial h}{\partial t}+\frac{\partial hU}{\partial x}=0\\&\frac{\partial hU}{\partial t}+\frac{\partial}{\partial x}\left(hU^2+\frac{gh^2}{2}+h^3\varphi+hP\right)=\frac{\partial}{\partial x}\left(\frac{2h^3\sqrt{\varphi}}{R}\frac{\partial U}{\partial x}\right)-gh\frac{\partial b}{\partial x}\\&\frac{\partial hW}{\partial t}+\frac{\partial hUW}{\partial x}=\frac{3}{2}P-\frac{6hW\sqrt{\varphi}}{R}\\&\frac{\partial hP}{\partial t}+\frac{\partial hUP}{\partial x}=-a^2\left(h\frac{\partial U}{\partial x}+2W\right)\\&\frac{\partial h\varphi}{\partial t}+\frac{\partial hU\varphi}{\partial x}=-C_r h\varphi^{3/2}+\frac{4h\sqrt{\varphi}}{R}\left(\frac{\partial U}{\partial x}\right)^2+\frac{16W^2\sqrt{\varphi}}{hR}\end{aligned}\tag{21}$$

where we have used the relation $W=-\dfrac{h}{2}\dfrac{\partial U}{\partial x}+\text{small terms}$, for the source terms in the third and the last equations.

II – Model analysis

II – 1 Eigenstructure

Using the primitive form of the system (21), we define the Jacobian matrix as

$$\begin{pmatrix} U & h & 0 & 0 & 0 \\ g + 3h\varphi + \dfrac{P}{h} & U & 0 & 1 & h^2 \\ 0 & 0 & U & 0 & 0 \\ 0 & a^2 & 0 & U & 0 \\ 0 & 0 & 0 & 0 & U \end{pmatrix} \tag{22}$$

The eigenvalues are $\lambda = U$(triple roots), $U \pm \sqrt{gh + 3h^2\varphi + P + a^2}$. We note that the corresponding eigenvectors form a basis. This makes the matrix (22) diagonalizable and hence guarantees the hyperbolicity of the system (21).

II – 2 Dispersive properties

To derive the linear dispersive relation associated to the system (21) without dissipation and over the flat bottom, we linearize the equations around the equilibrium state $(h_0,\ U_0 = 0,\ W_0 = 0,\ P_0 = 0,\ \varphi_0)$ with respect to small perturbations $(h_1, U_1, W_1, P_1, \varphi_1)$:

$$h = h_0 + \varepsilon h_1,\ U = \varepsilon U_1,\ W = \varepsilon W_1,\ P = \varepsilon P_1,\ \varphi = \varphi_0 + \varepsilon\varphi_1.$$

We are looking for the harmonic wave solutions in the following form

$$(h_1, U_1, W_1, P_1, \varphi_1)^\top = (A_1, A_2, A_3, A_4, A_5)^\top e^{i(kx-\omega t)}. \tag{23}$$

Substituting (23) into the linearised equation leads to the dispersive relation

$$\frac{h_0^2}{3a^2}\omega^4 - \omega^2\left[1 + \frac{h_0^2k^2}{3}\left(1 + \frac{gh_0}{a^2}\right)\right] + gh_0k^2 = 0. \tag{24}$$

The complete dispersive relation can be solved explicitly as

$$\omega^2 = \frac{1}{2}\left[\frac{3a^2}{h_0^2} + a^2k^2\left(1 + \frac{gh_0}{a^2}\right) \pm \sqrt{\left(\frac{3a^2}{h_0^2} + a^2k^2\left(1 + \frac{gh_0}{a^2}\right)\right)^2 - \frac{12a^2gk^2}{h_0}}\right], \tag{25}$$

which is independent of φ_0. Note that as $a \to \infty$, the dispersive relation of (24) approaches to that of Serre-Green-Naghdi equation $\omega^2 = gh_0k^2/(1 + h_0^2k^2/3)$.

Another important characteristic of dispersive systems for water waves is the existence of solitary wave solutions. A solitary wave is a self-similar solution which propagates at a constant velocity c. The phase portrait analysis associated with system (21) when assuming no dissipation and a flat bottom allows us to show that this system admits such a type of solutions.

III – Numerical scheme

To obtain a second order accuracy, the second order in space is implemented with a finite volume MUSCL scheme. For the second order in time, we use the IMEX ARS2(2,2,2) scheme.

Let $\mathbf{q} = (h, hU, hW, hP, h\varphi)^\top$. System (21) can be written in a semi-discrete form as a sum of a slow part $s(\mathbf{q})$ and a fast part $f(\mathbf{q})$:

$$\mathbf{q}_t = s(\mathbf{q}) + f(\mathbf{q}), \tag{26}$$

where

$$s(\mathbf{q}) = -F(\mathbf{q})_x + \begin{pmatrix} 0 \\ \frac{\partial}{\partial x}\left(\frac{2h^3\sqrt{\varphi}}{R}\frac{\partial U}{\partial x}\right) - (hP)_x \\ -\frac{6hW\sqrt{\varphi}}{R} \\ 0 \\ -C_r h\varphi^{3/2} + \frac{4h\sqrt{\varphi}}{R}\left(\frac{\partial U}{\partial x}\right)^2 + \frac{16W^2\sqrt{\varphi}}{hR} \end{pmatrix},$$

$$f(\mathbf{q}) = \left(0,\, 0,\, \frac{3}{2}P,\, -a^2\left(h\frac{\partial U}{\partial x} + 2W\right),\, 0\right)^\top,$$

$$F(\mathbf{q}) = \left(hU,\, hU^2 + \frac{gh^2}{2} + h^3\varphi,\, hUW,\, hUP,\, hU\varphi,\, \right)^\top.$$

Let $\mathbf{Q}(t)$ be the approximation of the cell averages of $\mathbf{q}$. The IMEX ARS2(2,2,2) scheme consists of two explicit and two implicit stages. The first explicit stage is written as

$$\mathbf{Q}_1^\dagger = \mathbf{Q}^n + \gamma\Delta t s(\mathbf{Q}^n), \tag{27}$$

where $\gamma = 1 - \sqrt{2}/2$ and $\mathbf{Q}^n = \mathbf{Q}(t_n)$. Then, the intermediate state $\mathbf{Q}_1$ is solved implicitly from $\mathbf{Q}_1^\dagger$ by the first implicit stage

$$\mathbf{Q}_1 = \mathbf{Q}_1^\dagger + \gamma\Delta t f(\mathbf{Q}_1). \tag{28}$$

The second explicit stage is written as

$$(\mathbf{Q}^{n+1})^\dagger = \mathbf{Q}^n + \delta\Delta t s(\mathbf{Q}^n) + (1-\delta)\Delta t s(\mathbf{Q}_1) + (1-\gamma)\Delta t f(\mathbf{Q}_1), \tag{29}$$

where $\delta = 1 - 1/(2\gamma)$. Finally, the update of the solution to next time step $\mathbf{Q}^{n+1}$ is solved implicitly from $(\mathbf{Q}^{n+1})^\dagger$ by the second implicit stage

$$\mathbf{Q}^{n+1} = (\mathbf{Q}^{n+1})^\dagger + \gamma\Delta t f(\mathbf{Q}^{n+1}). \tag{30}$$

Using the analytical solution from the previous section we confirm the convergence order of the proposed numerical algorithm.

III – 1 Breaking criteria

The enstrophy φ plays an important role in determining the moment of wave breaking as it propagates close to the shore. The breaking point is characterized by a sudden increase of the enstrophy. This idea allows us to determine an appropriate threshold value φ_0 for the maximal value of enstrophy in order to determine the moment when turbulent viscosity should be activated.

For a solitary wave we introduce the nonlinearity parameter $\delta = a^*/h_0^*$ where a^* is the amplitude of the initial wave and h_0^* is the still water level. Note that when $\delta < 0.05$, the model (21) can be used directly *without any breaking criterion* ($\varphi_0 = 0$). However, for solitary waves with a nonlinearity $\delta > 0.05$, the enstrophy is still a relevant quantity for breaking but its values are not small enough before breaking to be entirely negligible and the turbulent viscosity should be activated only when the breaking is likely to occur. In this case the choice of the threshold depends on the nonlinearity parameter (as in [8]) :

$$\tilde{\varphi}_0 = \left(0.1 + \frac{0.031}{\delta}\right), \ \varphi_0 = \frac{g}{h_0^*}\tilde{\varphi}_0$$

Following [8], we chose the parameters C_r and R as follow $C_r = 0.48$, $R = \begin{cases} 1.7, & \delta > 0.05 \\ 6, & \delta < 0.05 \end{cases}$

Note that here the threshold value φ_0 and turbulent Reynold's number R are depending on the initial nonlinearity parameter δ, which may not be robust in the operational context. A new local criterion is under development.

III – 2 Experimental comparison

The new model (21) is validated by comparison with the experimental data from Hsiao *et al.* [7]. A solitary wave of amplitude a^* propagates over the topography of slope β with $\tan\beta = 1/60$ with a given still water level h_0^*. In the given experiment wave gauges measure a free surface elevation in time at different locations along the 300 m channel (14 trials with different a^* and h_0^* were compared in total). We provide several comparison for this time series data, using the parameters given above. The results are presented on Figure 2. In trial 3, $\delta = 0.048 < 0.5$, so no breaking criterion is used. Although the numerical breaking point at $x = 116.4$ m which is very close to the real breaking point at $x = 116.7$ m, we observe that there's a phase shift in the comparison which indicates that the numerical wave propagates slower than the experimental one. This discrepancy is small and acceptable. In trial 41, $\delta = 0.137 > 0.05$, the criterion is applied. In this trial, we have much better results. The numerical breaking point is at $x = 148.7$ m compare to the real breaking point at $x = 148$ m, the numerical propagation speed is in a good agreement with experimental one. We must note that the amplitude smaller than the experimental one just before breaking (e.g. see, Trial 3 ($x = 116.54$ m) or Trial 41($x = 150$ m) is due to a weakness of Green-Naghdi model for description of strongly nonlinear effects.

IV – Numerical scheme and implementation in Tolosa

We have found that the scheme (27)-(30) proposed for the numerical implementation of the new model is not always stable, and a more robust strategy is required. Moreover, we have recently shown that the hyperbolic structure of the model can be exploited to guarantee the stability of the approximations (in the sense of discrete energy decay). The

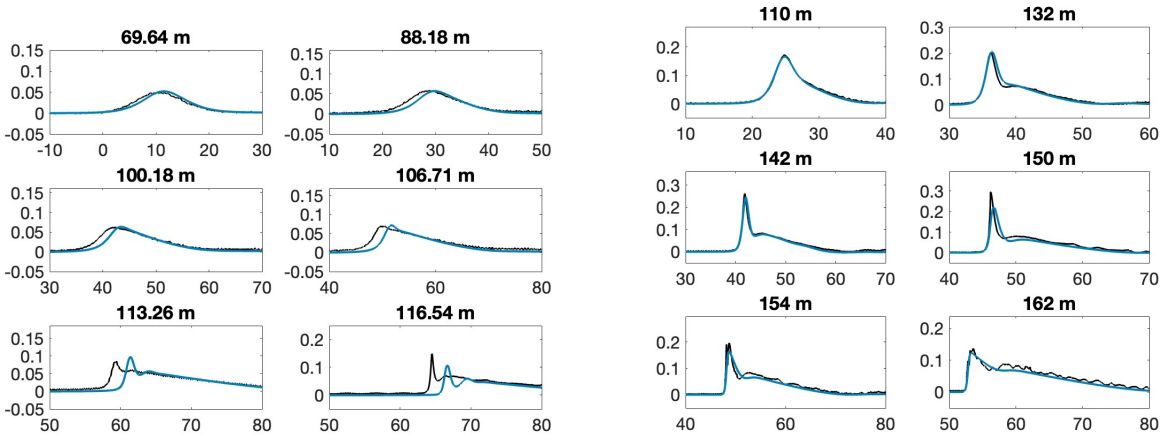

FIGURE 2 – Comparison of numerical (blue line) and experimental (black line) time series Trial 3 (left) and Trial 41 (right).

new numerical approach is first studied, on a flat bottom and without taking into account the enstrophy. The model we consider is the following

$$\begin{cases} \dfrac{\partial h}{\partial t} + \mathbf{div}(h\boldsymbol{U}) = 0\,, \\ \dfrac{\partial h\boldsymbol{U}}{\partial t} + \mathbf{div}\left[h\boldsymbol{U}\otimes\boldsymbol{U} + \left(\dfrac{1}{2}gh^2 + hP\right)\boldsymbol{I}\right] = 0\,, \\ \dfrac{\partial hW}{\partial t} + \mathbf{div}(h\boldsymbol{U}W) = \dfrac{3}{2}P\,, \\ \dfrac{\partial hP}{\partial t} + \mathbf{div}(h\boldsymbol{U}P) = -a^2\left(2W + h\ \mathbf{div}(\boldsymbol{U})\right)\,. \end{cases} \tag{31}$$

with the total energy conservation

$$\frac{\partial E}{\partial t} + \mathbf{div}\left(\left(E + \frac{1}{2}gh^2 + hP\right)\boldsymbol{U}\right) = 0\,, \tag{32}$$

where $\boldsymbol{I}$: Identity tensor, and $E = \dfrac{1}{2}h\left\|\boldsymbol{U}\right\|^2 + \dfrac{2}{3}hW^2 + \dfrac{1}{2}gh^2 + \dfrac{1}{2a^2}hP^2$.

The hyperbolic nature of the model provides an appropriate framework for the construction of a numerical scheme : absence of elliptic phase, existence of adapted methods for hyperbolic problems, propensity for parallelization. As a matter of fact, this structure allows to get rid of most of the limitations due to the existing strategies based on direct approaches for SGN equations. In particular, this structure can be exploited to guarantee the stability of the approximations in the sense of discrete energy decrease. On this basis, it is actually possible to propose several variants of energetically stable and low-diffusive numerical schemes on unstructured meshes, exhibiting an excellent compromise between accuracy and algorithmic complexity. These results are fundamental in the targeted application contexts. In the perspective of the construction of a numerical scheme, the model (31) can be recast under an appropriate split form. The first step reduces to a simple shallow water system with source term :

$$\left\{\begin{array}{l} \dfrac{\partial h}{\partial t} + \mathbf{div}(h\boldsymbol{U}) = 0\,, \\ \dfrac{\partial h\boldsymbol{U}}{\partial t} + \mathbf{div}\left(h\boldsymbol{U}\otimes\boldsymbol{U} + \dfrac{1}{2}gh^2\boldsymbol{I}\right) = 0\,, \\ \dfrac{\partial hW}{\partial t} + \mathbf{div}(h\boldsymbol{U}W) = 0\,, \\ \dfrac{\partial hP}{\partial t} + \mathbf{div}(h\boldsymbol{U}P) = 0\,. \end{array}\right. \tag{33}$$

admitting the following energy budget :

$$\frac{\partial E}{\partial t} + \mathbf{div}\left(\left(E + \frac{1}{2}gh^2\right)\boldsymbol{U}\right) = 0\,, \tag{34}$$

The second step of the splitting contains the acoustic contributions and can ve written :

$$\left\{\begin{array}{l} \dfrac{\partial h}{\partial t} = 0\,, \\ \dfrac{\partial \boldsymbol{U}}{\partial t} + \dfrac{1}{h}\mathbf{div}(hP) = 0\,, \\ \dfrac{\partial W}{\partial t} = \dfrac{3}{2}\dfrac{P}{h}\,, \\ \dfrac{\partial P}{\partial t} = -a^2\left(2\bar{W} + h\mathbf{div}(\boldsymbol{U})\right)\,. \end{array}\right. \tag{35}$$

The energy equation associated with this second part is :

$$\frac{\partial E}{\partial t} + \mathbf{div}\left(hP\boldsymbol{U}\right) = 0\,. \tag{36}$$

Regarding the hyperbolic phase (33), modern techniques dedicated to hyperbolic problems [1, 3] can be adapted to ensure a discrete counterpart of (34), while minimizing diffusive losses. At the numerical level, this step results in a state $\mathbf{Q} = (\bar{h}, \bar{\boldsymbol{U}}, \bar{W}, \bar{P})$ which will have to evolve through the second stage. The water height being constant through this step, we propose a discretization of the form :

$$\left\{\begin{array}{l} \boldsymbol{U}_K^{n+1} = \bar{\boldsymbol{U}}_K - \dfrac{\Delta t}{\bar{h}_K}\nabla_K[\bar{h}P^{n+1}]\,, \\ W_K^{n+1} = \bar{W}_K + \dfrac{3}{2}\Delta t\dfrac{P_K^{n+1}}{\bar{h}_K}\,, \\ P_K^{n+1} = \bar{P}_K - a^2\Delta t\left(2\dfrac{W_K^{n+1}}{\bar{h}_K} + \nabla_K\cdot[\bar{\boldsymbol{U}}^n]\right)\,. \end{array}\right. \tag{37}$$

Although appearing in implicit form the quantities W_K^{n+1} and P_K^{n+1} can be solved explicitely since they do not intervene in differential form in the source terms of the two last equations. This allows in a second time an explicit treatment of the velocity equation. The discrete opearator ∇_K is centred and it is actually possible to define the discrete divergence $\nabla_K\cdot$ in order to control the energy balance (36) of the second part. This approach will be used for implementation in Tolosa-project (tolosa-project.com).

V – Conclusions ans Perspectives

We have derived a new hyperbolic model which is capable to describe wave breaking in the surf zone. The mechanism of wave breaking is related to the emergence of large-scale

turbulence. This is accounted for by introducing a new variable enstrophy in addition to water depth and average flow velocity. The new model is validated by comparison with experiment [7]. Numerical results are in good agreement with experimental data.

However, the breaking criterion proposed in [8] and used here is not local and a new strategy is required. Moreover, no attempt is made here to improve the dispersive properties. The model is fully nonlinear and has the same dispersive properties as the classical Serre-Green-Naghdi equations. Using the idea introduced in [10], we can improve the dispersive properties.

Références

[1] C. Berthon, A. Duran, and K. Saleh. An easy control of the artificial numerical viscosity to get discrete entropy inequalities when approximating hyperbolic systems of conservation laws. *Continuum Mechanics, Applied Mathematics and Scientific Computing : Godunov's Legacy - Springer Nature Switzerland AG*, 55(12), 2020.

[2] A. Duran, F. Marche, R. Turpault, and C. Berthon. Asymptotic preserving scheme for the shallow water equations with source terms on unstructured meshes. *J. Comput. Phys.*, 287 :184–206, 2015.

[3] A. Duran, J. Vila, and R. Baraille. Energy-stable staggered schemes for the shallow water equations. *J. of Comp. Phys.*, 55(12) :401, 2020.

[4] C. Escalante, M. Dumbser, and M. Castro. An efficient hyperbolic relaxation system for dispersive non-hydrostatic water waves and its solution with high order discontinuous galerkin schemes. *J. Comput. Phys.*, 394 :385–416, 2019.

[5] C. Escalante and T. Morales de Luna. A general non-hydrostatic hyperbolic formulation for boussinesq dispersive shallow flows and its numerical approximation. *J. Sci. Comput.*, 83 :1–37, 2020.

[6] N. Favrie and S. Gavrilyuk. A rapid numerical method for solving serre–green–naghdi equations describing long free surface gravity waves. *Nonlinearity*, 30(7), 2017.

[7] S. C. Hsiao, T. W. Hsu, T. C. Lin, and Y. H. Chang. On the evolution and run-up of breaking solitary waves on a mild sloping beach. *Coast. Engrg*, 55(12) :975–988, 2008.

[8] M. Kazakova and G. L. Richard. A new model of shoaling and breaking waves : one-dimensional solitary wave on a mild sloping beach. *Journal of Fluid Mechanics*, 862 :552–591, 2019.

[9] A. Kennedy, Q. Chen, J. Kirby, and A. Dalrymple. Boussinesq modeling of wave transformation, breaking and runup. i :1d. journal of waterway, port, coastal and ocean engineering. *J. of waterway, port, coastal and ocean engineering*, 125(1), 2000.

[10] G. L. Richard. An extension of the boussinesq-type models to weakly compressible flows. *European Journal of Mechanics - B/Fluids*, 89 :217–240, 2021.

[11] G. L. Richard, A. Duran, and B. Fabrèges. A new model of shoaling and breaking waves. part ii. run-up and two-dimensional waves. *Journal of Fluid Mechanics*, 867 :146–194, 2019.

[12] V. M. Teshukov. Gas-dynamics analogy for vortex free-boundary flows. *J. Applied Mechanics and Technical Physics*, 48 :303–309, 2007.

[13] M. Tissier, P. Bonneton, F. Marche, F. Chazel, and D. Lannes. A new approach to handle wave breaking in fully non-linear boussinesq models. *Coastal Engineering*, 67 :54–66, 2012.